

This item is likely protected under Title 17 of the U.S. Copyright Law. Unless on a Creative Commons license, for uses protected by Copyright Law, contact the copyright holder or the author.

Access to this work was provided by the University of Maryland, Baltimore County (UMBC) ScholarWorks@UMBC digital repository on the Maryland Shared Open Access (MD-SOAR) platform.

Please provide feedback

Please support the ScholarWorks@UMBC repository by emailing scholarworks-group@umbc.edu and telling us what having access to this work means to you and why it's important to you. Thank you.

CORRELATED RADIO–X-RAY VARIABILITY OF GALACTIC BLACK HOLES: A RADIO–X-RAY FLARE IN CYGNUS X-1

JÖRN WILMS,¹ KATJA POTTSCHMIDT,² GUY G. POOLEY,³ SERA MARKOFF,⁴ MICHAEL A. NOWAK,⁵

INGO KREYKENBOHM,^{6,7} AND RICHARD E. ROTHSCCHILD²

Received 2007 April 10; accepted 2007 May 30; published 2007 June 22

ABSTRACT

We report on the first detection of a quasi-simultaneous radio–X-ray flare of Cygnus X-1. The detection was made on 2005 April 16 with pointed observations by the *RXTE* and the Ryle telescope, during a phase where the black hole candidate was close to a transition from its soft state to its hard state. The radio flare lagged the X-rays by ~ 7 minutes, peaking at 3:20 hr barycentric time (TDB 2,453,476.63864). We discuss this lag in the context of models explaining such flaring events as the ejection of electron bubbles emitting synchrotron radiation.

Subject headings: accretion, accretion disks — black hole physics — X-rays: binaries — X-rays: stars

Online material: color figure

1. INTRODUCTION

With the increased availability of simultaneous radio and observations in the last decade, there is now a large amount of evidence available pointing toward a very close interaction between the accretion disk and the jet in black hole X-ray binaries and active galactic nuclei. Most convincingly, this disk-jet interaction has been shown for microquasars, i.e., black hole binaries with strongly relativistic jets such as GRS 1915+105 or GRO J1655–40. In these systems, the correlated flaring in the X-rays, optical/infrared, and radio seen at certain times is generally interpreted as the evidence for (ballistic) ejection events of synchrotron radiation–emitting electron bubbles (Rothstein et al. 2005; Fender & Belloni 2004; Klein-Wolt et al. 2002; Eikenberry et al. 1998 and therein). In this model, the X-ray flare represents the ejection of the synchrotron radiation–emitting bubble, which then adiabatically expands within the jet flow and cools down, resulting in the peak of the emission shifting downward in frequency with time (van der Laan 1966; Hjellming & Johnston 1988). Simultaneous broadband observations of such events, which show minute-long delays between the different wave bands, are consistent with this picture (Mirabel & Rodríguez 1994; Mirabel et al. 1998; Pooley & Fender 1997; Eikenberry et al. 1998). The model has also been confirmed by proper-motion measurements in the radio, which reveal intrinsic jet speeds of $\geq 0.57c$ for GRS 1915+105 (Miller-Jones et al. 2005). Comparable behavior was also detected in 3C 120, suggesting that similar ejections also occur in active galactic nuclei, on correspondingly longer timescales (Marscher et al. 2002).

For black hole binaries with weakly relativistic jets, the evi-

dence for jet-disk interaction is less direct. This evidence includes the correlation between X-ray states and radio emission in black hole transients (e.g., in GX 339–4; Corbel et al. 2003; Belloni et al. 2005) and the success of modeling the radio–X-ray broadband spectrum of black hole candidates with outflow-dominated models (Markoff et al. 2005; Markoff & Nowak 2004 and therein). Furthermore, at least for Cygnus X-1, there is also evidence for the presence of an energetically significant, strong outflow (Stirling et al. 1998, 2001; Gallo et al. 2005; Miller-Jones et al. 2006). A relativistic jet with $v \geq 0.3c$ has been associated with radio flares in this system (Fender et al. 2006).

Apart from GRS 1915+105, however, none of these observations show direct evidence for a causal connection between the X-rays and the jet on timescales of minutes. Prompted by this lack of quasi-simultaneous short-term radio–X-ray correlations, in 1998 we initiated a long-term monitoring campaign of Cyg X-1 with the *Rossi X-Ray Timing Explorer* (*RXTE*) and the Ryle telescope. Biweekly 3–10 ks–long simultaneous observations started in 1999. Previous searches for flares in campaign data taken between 1999 and mid-2003 did not reveal evidence for coherent short-term activity in both bands, although a significant correlation on timescales of weeks was found, especially above ~ 10 keV (Gleissner et al. 2004; Wilms et al. 2006). In this Letter, we report on the observation made on 2005 April 16, in which the first clear quasi-simultaneous radio–X-ray flare was detected in Cyg X-1. The remainder of this Letter is structured as follows. In § 2 we describe the observations, followed by the analysis of the flare in § 3. We discuss the physics of the flare in the context of emission models for the radio and X-ray emission in § 4.

2. OBSERVATIONS AND DATA REDUCTION

We use data from both instruments on board the *RXTE*, the low-energy Proportional Counter Array (PCA; Jahoda et al. 2006) and the High Energy X-Ray Timing Experiment (HEXTE; Rothschild et al. 1998). The data analysis was performed using the standard *RXTE* data analysis software, HEASOFT 6.1.2. Spectral fitting was performed with XSPEC 11.3.2aa (Arnaud 1996).

A crucial part of the observation happened during the early phase of the *RXTE* observation, shortly after the source rose above the Earth’s horizon. Due to auroral emission in the far-ultraviolet and soft X-rays and due to cosmic-ray reprocessing in the hard X-rays, the Earth’s atmosphere is not completely X-ray dark. The

¹ Dr. Karl Remeis-Observatory, University of Erlangen-Nuremberg, Sternwartstrasse 7, 96049 Bamberg, Germany; joern.wilms@sternwarte.uni-erlangen.de.

² Center for Astrophysics and Space Sciences, University of California, San Diego, La Jolla, CA 92093-0424; kpottschmidt@ucsd.edu, rrothschild@ucsd.edu.

³ Mullard Radio Astronomy Observatory, Cavendish Laboratory, Madingley Road, Cambridge CB3 0HE, UK; guy@mrao.cam.ac.uk.

⁴ Astronomical Institute “Anton Pannekoek,” University of Amsterdam, Kruislaan 403, Amsterdam, 1098 SJ, Netherlands; sera@astro.uva.nl.

⁵ MIT Kavli Institute for Astrophysics and Space Research and *Chandra* X-Ray Center, NE80-6077, 77 Massachusetts Avenue, Cambridge, MA 02139; mnowak@alum.mit.edu.

⁶ Institut für Astronomie und Astrophysik—Astronomie, Sand 1, 72076 Tübingen, Germany; kreyken@astro.uni-tuebingen.de.

⁷ INTEGRAL Science Data Centre, Chemin d’Écogia 16, 1290 Versoix, Switzerland.

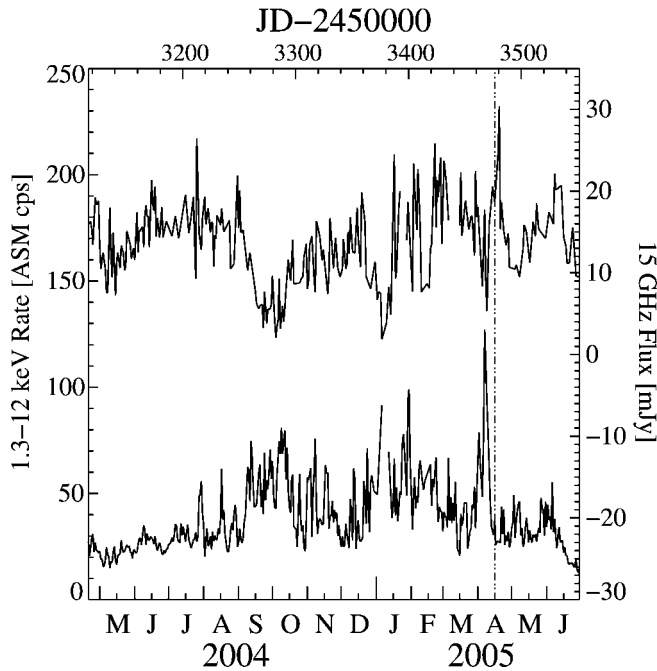


FIG. 1.—*RXTE* ASM (lower curve, left y-axis) and Ryle telescope 15 GHz (upper curve, right y-axis) light curves of Cyg X-1 from 2004 March until 2005 June. The time of the simultaneous observation is indicated by the dotted vertical line. Gaps are shown if their duration is ≥ 4 days.

typical 2.5–20 keV X-ray flux at the typical magnetic latitude of the *RXTE* orbit is too low, however, to influence our measurements (Petrinec et al. 2000; Sazonov et al. 2007). We therefore use all data taken while the source was $\geq 1^\circ$ above the Earth's horizon and had a source offset of $\leq 0.01^\circ$. We use PCA data from the standard1 mode, which gives the full 2.5–128 keV PCA count rate with a time resolution of 0.125 s and no energy information, and from the standard2f mode, a binned data mode with a 128 channel energy resolution and a time resolution of 16 s. X-ray light curves were extracted with the intrinsic time resolution of each mode and then barycentered and rebinned.

The Ryle telescope data were taken at 15 GHz with a time resolution of ~ 8 s. The typical 1σ uncertainty of the radio measurements is 9 mJy. The observations are interrupted every ~ 1600 s for phase-calibration observations of J2007+4029. The amplitude calibration of the Ryle data corresponds to the flux scale of Baars et al. (1977) and is performed using nearby observations of 3C 48 and 3C 286. See Pooley & Fender (1997) for further information on the Ryle telescope.

3. A QUASI-SIMULTANEOUS RADIO-X-RAY FLARE

As shown in Figure 1, 2005 April marks the possible end of a longer X-ray flaring episode of Cyg X-1 that started in early 2004 (Wilms et al. 2006). While clearly defined radio flares are not uncommon in Cyg X-1 (e.g., Hjellming 1973), increased radio emission and radio flaring are generally seen when the source is in the intermediate state between the hard and soft states, while the radio is weak once the X-ray source approaches the soft state (Wilms et al. 2006 and therein). At the time of our pointed observations, the soft X-ray flux had just come down from a large flare. Shortly after the observation, the 1 day averaged 15 GHz flux peaked, reaching a maximum of ~ 30 mJy, close to the brightest radio flux of Cyg X-1 during 2004/2005.

Figure 2 shows the 15 GHz radio flux and the *RXTE* PCA count rate light curve measured on 2005 April 16. Close to the start of the observation, a radio flare is readily apparent.

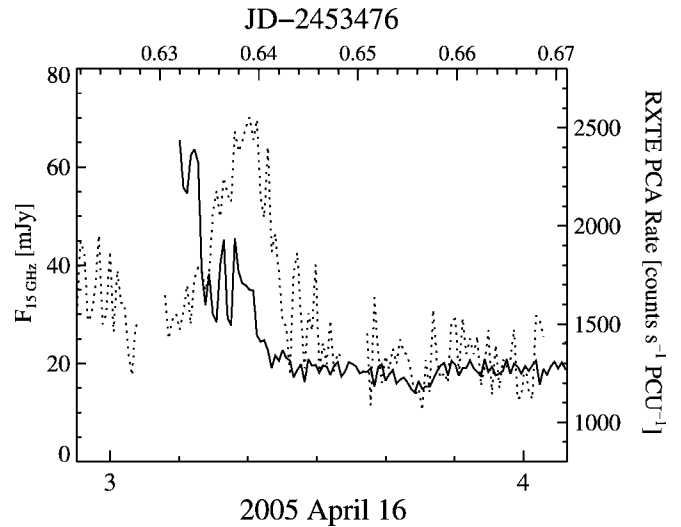


FIG. 2.—Barycentric 15 GHz flux density (left axis, dotted line) and 2–128 keV count rate light curves (right axis, solid line) of Cyg X-1 for the flare event of 2005 April 16, both binned to a resolution of 32 s. The bottom axis gives the barycentric time in hours, with tick marks separated by 10 minutes.

The total duration of the flare is ~ 15 minutes. During this interval, the 15 GHz flux increased by a factor of ~ 3 to a peak radio flux of 70 mJy. This radio flux is among the highest seen during the Ryle monitoring.⁸ Previous radio flares, however, did not occur during pointed *RXTE* observations (Gleissner et al. 2004; Fender et al. 2006), and the source monitoring provided by the *RXTE* All-Sky Monitor (ASM) is too coarse to pick up such short-lived X-ray events.

RXTE started observing Cyg X-1 about 10 minutes before the peak radio flux. The X-ray light curve shown in Figure 2 shows a similar shape to the radio one, although with more substructure. The earlier maximum of the X-ray flare did not allow *RXTE* to catch the start of the X-ray flare, or to determine whether or not the maximum X-ray flux seen is indeed the peak of the X-ray flare. A cross correlation function (CCF) analysis using the algorithm of Scargle (1989) reveals a 413 ± 165 s time lag of the radio with respect to the X-rays, where the 1σ uncertainty was determined using a standard bootstrapping method with 1000 realizations. Other approaches to calculate the CCF for nonuniformly sampled data (Alexander 1997; Edelson & Krolik 1988) give essentially the same result. With a maximum Scargle (1989) CCF of 0.38, this analysis formally confirms the general similarity of the X-ray and radio light curves (Fig. 3). Since the substructure of the X-ray light curve, i.e., the two smaller flares after the main flare, is clearly different from that in the radio flare, and since the start of the X-ray flare is not covered by our observations, the peak CCF value is not higher. For the same reasons, the formal uncertainty of the lag measurement is rather large.

To characterize the shape of the radio flare, we fit the radio data (rebinned to a resolution of 8 s) with the sum of a linear flux trend and a Gaussian representing the flare,

$$f(t) = a(t - t') + b + A \exp \left[-\frac{(t - T)^2}{\sigma^2} \right], \quad (1)$$

where t' is a reference time, taken as the center of the time

⁸ The most exceptional radio flare was that of 2004 February 20, which reached a peak flux of 140 mJy at 15 GHz, the largest flux ever seen for this source with the Ryle telescope (Fender et al. 2006).

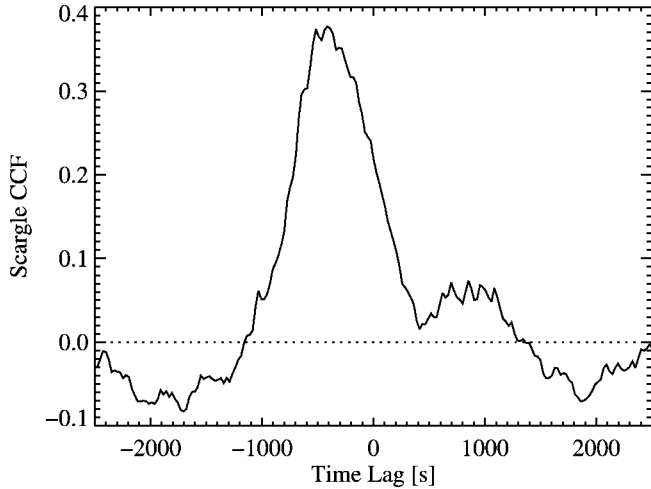


FIG. 3.—CCF (Scargle 1989) for the radio data with respect to the *RXTE*-PCA data. A negative time lag indicates the radio lagging the X-rays.

interval analyzed ($t' = \text{JD } 2,453,476.64635$). The barycentric time of maximum flux occurred at $T = \text{JD } 2,453,476.63864$ with an uncertainty of 15 s (uncertainties are at the 1σ level for one interesting parameter). The peak flux of the flare component is $A = 39.2 \pm 2.5$ mJy, and the width of the component is $\sigma = 210 \pm 16$ s. The flare is superimposed to a continuum with $b = 25.3 \pm 0.7$ mJy, decreasing linearly with $a = -13 \pm 2$ mJy hr^{-1} . The high quality of the fit is indicated by its low reduced χ^2 ($\chi^2_{\text{red}} = 1.11$ for 233 degrees of freedom). The radio flare is therefore symmetric around its maximum, and this symmetry is what makes it markedly different from the asymmetric flare of 2004 February 20 (Fender et al. 2006).

Modeling the *RXTE*-PCA light curve is complicated by the flare already being in progress when the measurements started. Furthermore, contrary to the radio data, where the scatter in the light curve is mainly due to the measurement uncertainty, the X-ray data are dominated by strong low-frequency noise onto which the X-ray flare is superimposed. Consequently, the empirical model of equation (1) does not result in a good description of the X-ray data.

To study the spectral evolution of Cyg X-1 during the flare, we perform a spectral analysis of the 2.5–20 keV PCA standard2f data at 16 s time resolution using a simple photoabsorbed power law, which proves sufficient to describe the spectrum at this lower signal-to-noise ratio level. For spectra taken during the flare, at PCA count rates above 1000 counts s^{-1} PCU^{-1} , the mean power-law index $\Gamma = 2.10 \pm 0.03$. The spectrum hardens outside of the flare to $\Gamma = 1.98 \pm 0.03$ (errors given are the standard deviation of the individual power-law fits to the standard2f spectra), a value typical for the intermediate state of this source (Wilms et al. 2006).

That Cyg X-1 was in the intermediate state on the day of the flare can also be confirmed by modeling the 2.5–150 keV PCA and HEXTE spectrum of an *RXTE* observation performed 4 hr after the flare (to avoid possible “contamination” by the flaring activity) with the sum of a photoabsorbed ($N_{\text{H}} = 6 \times 10^{21} \text{ cm}^{-2}$, held fixed), exponentially cutoff broken power-law model. This empirical model has been shown to give a good characterization of the spectral shape of Cyg X-1 (Wilms et al. 2006). The spectral parameters are a lower photon index $\Gamma_1 = 2.01 \pm 0.01$, breaking at $E_{\text{break}} = 10.0^{+0.3}_{-0.2}$ keV into a power law with $\Gamma_2 = 1.62^{+0.02}_{-0.03}$. At $E_{\text{cut}} = 26 \pm 3$ keV, the exponential cutoff starts with a folding energy of $E_{\text{fold}} = 137 \pm 11$ keV (all uncertainties are at the 90% level). In addition, a Fe K α line from neutral iron is present with an equivalent

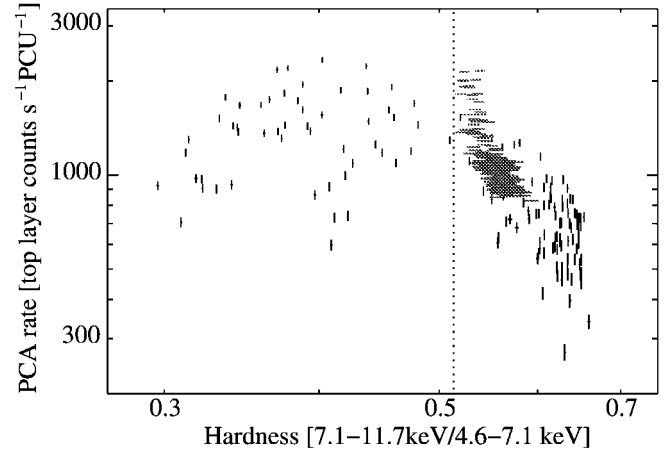


FIG. 4.—The 1–128 keV *RXTE*-PCA count rate vs. the hardness ratio for Cyg X-1 observations from the 2000–2005 *RXTE* monitoring (black error bars) and for data taken during the 2005 April 16 flare (gray bars). The dotted line indicates the location at which observations with maximum radio flux are found in the long-term monitoring. The hardness ratio was determined from background-subtracted PCA top-layer data from channels 8–14 and 15–25, respectively. [See the electronic edition of the *Journal* for a color version of this figure.]

width of 135 eV. The 3–10 keV source flux is 6.17×10^{-9} ergs $\text{cm}^{-2} \text{ s}^{-1}$. The parameters of the continuum are again consistent with an intermediate state and fit well with the empirical picture that radio flaring in black hole candidates occurs most frequently in this state (Fender et al. 2004; Wilms et al. 2006).

To allow the interpretation of the observed softening during the flare with the general behavior of Cyg X-1, Figure 4 shows the X-ray hardness intensity diagram for the PCA top-layer standard2f 16 s spectra in the context of the pointed *RXTE* observations of the monitoring campaign. For black hole transients, this diagram is seen to have an approximate q shape (Belloni et al. 2006 and therein). As a persistent hard-state source, Cyg X-1 is typically found in the top right-hand corner of the diagram. Outside of the flare, the source is situated at a hardness of ~ 0.55 with a typical 1–128 keV PCA count rate of ~ 900 counts s^{-1} PCU^{-1} . During the flare, the source softens and brightens. It leaves the region of the diagram where Cyg X-1 is usually found during our monitoring campaign, by moving to higher count rates, for this hardness, than usually observed.

Flaring behavior in Cyg X-1 is usually observed whenever the source is close to the “jet line” in its hardness intensity diagram, while the radio flux gets quenched once the source moves away from the jet line to the left of the diagram (Gallo et al. 2003; Fender et al. 2004). In spectral fits based on the *eqpair* model of Coppi (1999), the radio fluxes of Cyg X-1 are at their maximum when the compactness ratio $l_{\text{h}}/l_{\text{s}} \sim 3$ (Fig. 16 of Wilms et al. 2006; the compactness ratio is a measure for the relative importance of the energy dumped into the Comptonizing plasma and that dissipated in the accretion disk), corresponding to a soft power-law index of $\Gamma_1 \sim 2.1$. From our database of spectra of Cyg X-1, we find that these observations have a (7.1–11.7 keV)/(4.6–7.1 keV) hardness ratio of 0.52, indicated by the dotted line in Figure 4. During the 2005 April 16 observation, the source was therefore close to this line of maximum radio flux and approached it asymptotically during the flare.

4. DISCUSSION

In this Letter we have presented the first evidence for a direct relationship of the X-ray and radio emission in Cyg X-1 on timescales of minutes. The data show the radio to lag the X-rays by 413 ± 165 s and the X-ray spectral shape to approach

the X-ray hardness ratio where the source is typically found at its largest radio flux in our long-term monitoring, hinting toward a general similarity of the physics of individual flare events and the overall radio–X-ray connection. Although the X-ray data do not cover the start of the X-ray flare, explaining the rather large uncertainty of the lag determination, the morphological similarities between the X-ray and radio light curves also suggest that the same event is observed in both wave bands.

Similar events in microquasars show that lags with timescales of several hundred seconds are typical for the coherent behavior of these systems, such as a lag of 310 ± 20 s between the soft X-rays and the IR (Eikenberry et al. 1998), and 800 s between the X-rays and the radio (Pooley & Fender 1997), in GRS 1915+105. The timescale observed in Cyg X-1 allows us to place an upper limit on the physical separation of the X-ray–emitting and radio–emitting regions of the accretion/ejection flow. We assume that the emission coincides with the imaged jet and that the jet is perpendicular to the orbital plane of the HDE 226868/Cyg X-1 system (although this is not a priori certain; Maccarone 2002), which has an inclination of 30° (Gies & Bolton 1982; Dolan 1992). Taking light-travel time effects into account, for jet speeds of $0.3c$, the lower limit implied by observations of the transient jet ejection discussed by Fender et al. (2006), the measured delay implies a separation of 1.1 ± 0.5 AU between the location of X-ray emission and the location of radio emission. If the jet is relativistic instead, with a speed of $0.99c$, the distance increases to 5.8 ± 2.3 AU. Note that similar values for the length of the jet are obtained by considering that the ~ 10 minute duration of the radio flare is roughly equal to the dynamical timescale of the jet. Assuming a distance of 2.5 kpc, these values imply a maximum projected angular separation between the X-ray–emitting and radio–emitting region of 10^{-3} mas.

What is the physics of the observed event? In the model of Fender et al. (2004) for transient radio events, the inner edge of a thin accretion disk is posited to move rapidly toward the black hole. The temperature at the inner edge therefore in-

creases, leading to a softening of the source in the *RXTE* PCA as more disk photons enter the instrument’s bandpass. This X-ray flare is then followed by the ejection of an electron bubble, which rapidly expands, producing the observed radio emission. At least qualitatively, this behavior and also the timescales deduced above seem to agree with our observations, although the model was originally invented for the large-scale variability of black hole candidates and not for such short events as the one discussed here. Note that while the main flare dominates the measured time lag and therefore the sizes estimated above, it is followed by two short spikes, which are both present in the radio and the X-ray light curves, but at different time delays. These spikes could indicate that more than one blob of material was ejected at different speeds but that they cannot be separated once the blobs have expanded and their radiation peaks in the radio. Such a behavior could be typical for flares in Cyg X-1, since the large radio flare of Cyg X-1 from 2005 February 20 also shows very little substructure (Fender et al. 2006).

The lack of further detections of radio–X-ray flares in over 1.5 Ms of simultaneous radio–X-ray data precludes a more detailed discussion of the properties of the ejected material (from a comparison of the source behavior during different flares). The observation of the flare itself, however, stresses the importance of long-term multiwavelength campaigns to detect such rare events; these campaigns are necessary to further our insight into the physics of the emission from black holes.

We acknowledge the support of NASA contract NAS5-30720, NASA grant NNG05GK55G, and a travel grant from the Deutscher Akademischer Austauschdienst. We thank the *RXTE* schedulers for their efforts in making the simultaneous radio–X-ray observations possible and the Aspen Center for Physics for its hospitality during the early stages of the preparation of this manuscript.

Facilities: RXTE(PCA, HEXTE), Ryle

REFERENCES

- Alexander, T. 1997, in *Astronomical Time Series*, ed. D. Maoz, A. Sternberg, & E. M. Leibowitz (Dordrecht: Kluwer), 163
- Arnaud, K. A. 1996, in *ASP Conf. Ser. 101, Astronomical Data Analysis Software and Systems V*, ed. J. H. Jacoby & J. Barnes (San Francisco: ASP), 17
- Baars, J. W. M., Genzel, R., Pauliny-Toth, I. I. K., & Witzel, A. 1977, *A&A*, 61, 99
- Belloni, T., Homan, J., Casella, P., van der Klis, M., Nespoli, E., Lewin, W. H. G., Miller, J. M., & Méndez, M. 2005, *A&A*, 440, 207
- Belloni, T., et al. 2006, *MNRAS*, 367, 1113
- Coppi, P. 1999, in *ASP Conf. Ser. 161, High Energy Processes in Accreting Black Holes*, ed. J. Poutanen & R. Svensson (San Francisco: ASP), 375
- Corbel, S., Nowak, M. A., Fender, R. P., Tzioumis, A. K., & Markoff, S. 2003, *A&A*, 400, 1007
- Dolan, J. F. 1992, *ApJ*, 384, 249
- Edelson, R. A., & Krolik, J. H. 1988, *ApJ*, 333, 646
- Eikenberry, S. S., Matthews, K., Morgan, E. H., Remillard, R. A., & Nelson, R. W. 1998, *ApJ*, 494, L61
- Fender, R., & Belloni, T. 2004, *ARA&A*, 42, 317
- Fender, R. P., Belloni, T. M., & Gallo, E. 2004, *MNRAS*, 355, 1105
- Fender, R. P., Stirling, A. M., Spencer, R. E., Brown, I., Pooley, G. G., Muxlow, T. W. B., & Miller-Jones, J. C. A. 2006, *MNRAS*, 369, 603
- Gallo, E., Fender, R., Kaiser, C., Russell, D., Morganti, R., Oosterloo, T., & Heinz, S. 2005, *Nature*, 436, 819
- Gallo, E., Fender, R. P., & Pooley, G. G. 2003, *MNRAS*, 344, 60
- Gies, D. R., & Bolton, C. T. 1982, *ApJ*, 260, 240
- Gleissner, T., et al. 2004, *A&A*, 425, 1061
- Hjellming, R. M. 1973, *ApJ*, 182, L29
- Hjellming, R. M., & Johnston, K. J. 1988, *ApJ*, 328, 600
- Jahoda, K., Markwardt, C. B., Radeva, Y., Rots, A. H., Stark, M. J., Swank, J. H., Strohmayer, T. E., & Zhang, W. 2006, *ApJS*, 163, 401
- Klein-Wolt, M., Fender, R. P., Pooley, G. G., Belloni, T., Migliari, S., Morgan, E. H., & van der Klis, M. 2002, *MNRAS*, 331, 745
- Maccarone, T. J. 2002, *MNRAS*, 336, 1371
- Markoff, S., & Nowak, M. A. 2004, *ApJ*, 609, 972
- Markoff, S., Nowak, M. A., & Wilms, J. 2005, *ApJ*, 635, 1203
- Marscher, A. P., Jorstad, S. G., Gómez, J.-L., Aller, M. F., Teräsranta, H., Lister, M. L., & Stirling, A. M. 2002, *Nature*, 417, 625
- Miller-Jones, J. C. A., Fender, R. P., & Nakar, E. 2006, *MNRAS*, 367, 1432
- Miller-Jones, J. C. A., McCormick, D. G., Fender, R. P., Spencer, R. E., Muxlow, T. W. B., & Pooley, G. G. 2005, *MNRAS*, 363, 867
- Mirabel, I. F., Dhawan, V., Chaty, S., Rodríguez, L. F., Martí, J., Robinson, C. R., Swank, J., & Geballe, T. R. 1998, *A&A*, 330, L9
- Mirabel, I. F., & Rodríguez, L. F. 1994, *Nature*, 371, 46
- Petrinec, S. M., McKenzie, D. L., Imhof, W. L., Mobilia, J., & Chenette, D. L. 2000, *J. Atmos. Sol.-Terr. Phys.*, 62, 875
- Pooley, G. G., & Fender, R. P. 1997, *MNRAS*, 292, 925
- Rothschild, R. E., et al. 1998, *ApJ*, 496, 538
- Rothstein, D. M., Eikenberry, S. S., & Matthews, K. 2005, *ApJ*, 626, 991
- Sazonov, S., Churazov, E., Sunyaev, R., & Revnivtsev, M. 2007, *MNRAS*, 377, 1726
- Scargle, J. D. 1989, *ApJ*, 343, 874
- Stirling, A. M., Spencer, R. E., de la Force, C. J., Garrett, M. A., Fender, R. P., & Ogley, R. N. 2001, *MNRAS*, 327, 1273
- Stirling, A., Spencer, R., & Garrett, M. 1998, *NewA Rev.*, 42, 657
- van der Laan, H. 1966, *Nature*, 211, 1131
- Wilms, J., Nowak, M. A., Pottschmidt, K., Pooley, G. G., & Fritz, S. 2006, *A&A*, 447, 245